


## Article

# Urban Pluvial Flood Modeling by Coupling Raster-Based Two-Dimensional Hydrodynamic Model and SWMM

Quntao Yang <sup>1,2</sup> , Zheng Ma <sup>1,2</sup> and Shuliang Zhang <sup>1,2,\*</sup>

<sup>1</sup> Key Laboratory of VGE of Ministry of Education, Nanjing 210023, China; yang\_1990@outlook.com (Q.Y.); mzleman@126.com (Z.M.)

<sup>2</sup> School of Geography, Nanjing Normal University, Nanjing 210023, China

\* Correspondence: zhangshuliang@njnu.edu.cn

**Abstract:** Urban flood modeling usually involves simulating drainage network runoff and overland flow. We describe a method for urban pluvial flood modeling by coupling the stormwater management model (SWMM) with a raster-based 2D hydrodynamic model, which is based on a simplified form of the shallow water equations. Then, the method is applied to a highly urbanized area in Nanjing City, China. The elevation of the raster-based 2D hydrodynamic model shows that the raster-based model has comparable capabilities to LISFLOOD-FP for surface flood modeling. The calibration and validation results of the coupled model show that the method is reliable. Moreover, simulation results under the six rainfall return periods, which include 1-, 5-, 10-, 20-, 50-, and 100-year return periods show that node overflow, water depth, and flooding area increase proportionately as the intensity of rainfall increases. Therefore, the coupling model provides a simplified and intuitive method for urban pluvial flood modeling, which can be used to detect flood-sensitive areas and elevate the capacity of urban drainage networks for urban pluvial flooding.

**Keywords:** urban pluvial flood; 2D hydrodynamic model; coupled model; storm water management model



**Citation:** Yang, Q.; Ma, Z.; Zhang, S. Urban Pluvial Flood Modeling by Coupling Raster-Based Two-Dimensional Hydrodynamic Model and SWMM. *Water* **2022**, *14*, 1760. <https://doi.org/10.3390/w14111760>

Academic Editor: Wei Sun

Received: 21 April 2022

Accepted: 28 May 2022

Published: 30 May 2022

**Publisher's Note:** MDPI stays neutral with regard to jurisdictional claims in published maps and institutional affiliations.



**Copyright:** © 2022 by the authors. Licensee MDPI, Basel, Switzerland. This article is an open access article distributed under the terms and conditions of the Creative Commons Attribution (CC BY) license (<https://creativecommons.org/licenses/by/4.0/>).

## 1. Introduction

Urban flooding is among the most frequent and pervasive hazards resulting in substantial social and economic losses and impacting many cities worldwide [1]. Urban pluvial flooding is often caused by the insufficient capacity of municipal drainage systems, which cannot drain excess rainwater in a timely manner. Under rapid urbanization and global climate change, urban flooding is worsening [2–4]. Therefore, managing urban floods is crucial for global cities. Meanwhile, numerous measures, such as increasing drainage capacity and low-impact development (LID) methods, have been implemented to prevent or mitigate urban flooding [5]. However, the effective implementation of countermeasures and policies depends on understanding the hazard characteristics of urban floods, such as inundation extent and water depth. Therefore, flood modeling, which can reveal urban flood characteristics under different disaster scenarios, is an important method for managing urban floods [1].

Flood modeling is essential for simulating and expressing the characteristics of urban flood hazards and is frequently used in urban flood management and urban drainage system planning [3,6]. However, compared with the natural basin flood disaster simulation, the development and implementation of urban flood modeling are more complex because of the varying surface topography and drainage process [1,7,8]. The urban surface environment includes many buildings, roads, and different land-use classes with different water permeabilities. Moreover, in the process of urban rainfall-runoff, precipitation produces surface runoff, which can enter municipal sewer networks and become pipe runoff, eventually flowing into nearby rivers. Therefore, urban flood models not only need to simulate overland flow but also assist in the management of rainwater in urban drainage systems [7,8].

In the past decades, many flood models have been developed and specifically applied to urban areas, such as SWMM, InfoWorks ICM, and MIKE MOUSE [1]. In particular, the open-source SWMM model is widely used for urban pluvial flood modeling and urban drainage planning because of its ability to completely simulate the urban drainage process, even directly was used or borrowed by commercial software, such as InfoSWMM and MIKE MOUSE [9]. However, most of these urban storm management models are limited to the simulation of rainfall-runoff and urban drainage networks [10]. These models can simulate the drainage process of the urban drainage pipe network and the pipe points' overflow phenomenon. However, these models cannot express how the water overflow from the pipe network flows on the surface, a phenomenon that affects urban storm management and the assessment of urban flood impacts [10,11]. To overcome these models' deficiencies, many models later expanded the function of 2D surface simulation based on SWMM or other models, such as PCSWMM, MIKE Urban, and Sobek Urban [12–14]. However, the application of these commercial models or software in academic research is restricted due to copyright and high cost. Therefore, coupling a 2D hydrodynamic model to the open-source urban flood model, such as SWMM, is necessary for complete urban flood simulation.

Meanwhile, 2D hydrodynamic flood modeling, which is a common and well-established technology in flood or numerical calculation research [15,16], uses a grid as the basis for model simulation and result presentation [17]. Several types of grids, such as the triangle mesh and structured grid, are used in various flood models, and are generated by tools or using raster data directly [18–20]. In flood modeling, the generated grid has several advantages, most notably an unstructured mesh, which can represent the flood flow of roads similar to rivers or channels in urban areas [19]. However, compared with using raster data directly, models based on generated grids have a more challenging construction process, which needs to consider mesh generation, storage, the connection between grid and data, and data conversion to display the modeling results. Moreover, raster grids directly use Geographic Information System (GIS)-based data, such as the digital elevation model (DEM), which is handled by general GIS tools and programming languages such as ArcGIS Desktop, QGIS, MATLAB, and Python. Additionally, high-resolution raster data expresses the topographic features of buildings and roads and effectively simulates urban floods on the micro-scale. Currently, the improvement of computing power and the use of high-resolution terrain data that can express the urban surface has increased the popularity of 2D flooding inundation models such as LIFLOOD-FP and, Floodmap that are directly based on GIS terrain data [21,22].

This study implemented urban pluvial flood modeling by coupling the SWMM and a raster-based 2D hydrodynamic model, which can simulate the drainage network runoff and 2D surface flooding simultaneously in urban areas. In the model, the use of raster-based DEM can replace the process of mesh generation and terrain data fusion, which simplifies the model building process. Then, we selected an urban area in Nanjing City, China, which is crossed by the Yangtze River, as the case study area to calibrate and validate our model. Furthermore, we modeled urban pluvial floods in various rainfall scenarios to analyze the hazard characteristics of urban flooding in the study area.

The remainder of this article is organized as follows: the materials and methods, which include a description of the study area, available data, and methods, are introduced in Chapter 2, followed by the results section. Finally, the discussion and conclusions are presented.

## 2. Materials and Methods

### 2.1. Urban Flood Model

#### 2.1.1. SWMM Model

The SWMM developed by the US Environmental Protection Agency is a dynamic rainfall-runoff model applicable for simulating both single events and long-term performance of runoff quantity and quality for urbanized areas. The model has become one of the

best-known and most widely used urban flood models owing to its continued maintenance and updates [23].

In the flood modeling process, two primary components of the SWMM are used: the collection of rainfall and surface runoff and the routing of the drainage systems. In the SWMM, the surface is divided into units of different geometries and areas, called sub-catchments. These sub-catchments collect precipitation and excess rain to generate surface runoff. Moreover, the sub-catchments link to manholes or other drainage facilities. The surface runoff flows into sewer networks through pipes or channels and finally drains out of the urban drainage network. In this process, the SWMM uses a nonlinear reservoir model, a hydrological method, to estimate surface runoff. The 1D hydrodynamic model successfully simulates the urban drainage network; therefore, the SWMM model is a hydrology-hydraulics model.

For sewer network modeling, the SWMM supports different approaches, including steady flow, kinematic waves, and dynamic waves. The dynamic wave method solves the complete Saint-Venant equation (shallow water equation). The modeling results are theoretically the most accurate. Therefore, the dynamic wave method was chosen as the modeling method in this study, and the governing equations are written as follows:

$$\frac{\partial A}{\partial t} + \frac{\partial q}{\partial x} = 0, \quad (1)$$

$$\frac{\partial q}{\partial t} + \frac{\partial(q^2/A)}{\partial x} + \frac{gA\partial(h+z)}{\partial x} + \frac{gn^2q^2}{AR^{4/3}} = 0, \quad (2)$$

where  $A$  is the flow cross-sectional area;  $t$  is time;  $q$  is the flow rate or discharge in the pipes;  $g$  is the acceleration of gravity;  $h$  and  $z$  are the water depth and invert elevation in the pipes;  $n$  is the roughness coefficient of the pipes;  $R$  is the hydraulic radius of the flow cross-section.

In general, most urban flooding results from sewer overflows from manholes, when the pipe runoff exceeds the drainage capacity. Depending on whether surface ponding is allowed during modeling, the SWMM model has two ways to overflow from manholes as shown in Figure 1a,b, respectively. When surface ponding is not allowed, flooded water will be lost from the system as shown in Figure 1a. An alternative method is to assume that a specific ponding area can store these over-flows, which can flow into sewers again when the drainage capacity is restored (Figure 1b). Thus, neither method can reflect the surface flow formed by overflow from manholes, and cannot identify which buildings and facilities are affected by flooding. Integration of the 2D model is thus required to implement surface flow modeling, as shown in Figure 1c.

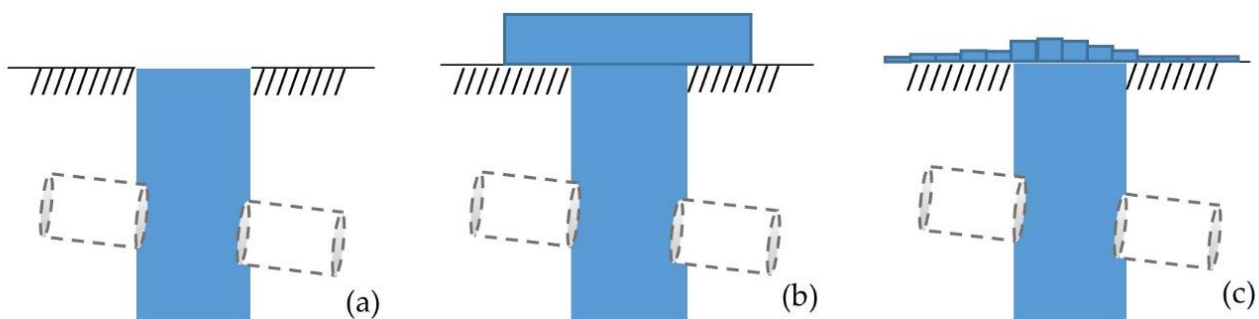


**Figure 1.** Three methods of sewer network surcharge in urban flood models: (a) when a manhole is not allowed to pond, flooded water will be lost from the system. (b) Flooded water can be stored in the ponding area and flow into sewers again when the drainage capacity is restored. (c) Integration of the 2D model is thus required to implement surface flow modeling. (a,b) The methods used in the SWMM, and method (c) is used in the 2D model.

### 2.1.2. Raster-Based 2D Flood Model

According to a current study, we developed a raster-based 2D hydrodynamic model to represent surface flooding in urban areas [23–25]. In the model, we assume that the floodplain is discretized by the raster grid, which leads to the possibility of using GIS-based DEM directly and replaces mesh generation in traditional hydrodynamic models, and simplifies the model building process. Cells in the DEM are treated as a series of storage cells that can exchange water with surrounding cells, representing the overland flow of the 2D model. The flow is calculated by a simple inertial formulation of the shallow water equations (Equations (5)–(7)), which are used in similar 2D flood inundation models, such as LISFLOOD-FP and Floodmap [21,22]. However, the 2D flood models only simulate the surface flow in the floodplain and handle the surcharge from the SWMM. They exclude the modeling of rivers and other infrastructures, such as weirs, bridges, and pipes.

In the simple formula, the momentum equation is shown in Equations (3)–(5), which neglects the advection term of the Saint-Venant or Shallow Water equations. For most flood modeling, the advection of surface flow is relatively unimportant, especially for urban flooding [21]. Meanwhile, the use of the simple formula increases the efficiency of the 2D model.

$$\frac{\partial h}{\partial t} + \frac{\partial q_x}{\partial x} + \frac{\partial q_y}{\partial y} = 0, \quad (3)$$

$$\frac{\partial q_x}{\partial t} + \frac{gh\partial(h+z)}{\partial x} + \frac{gn^2q^2}{hR^{4/3}} = 0, \quad (4)$$

$$\frac{\partial q_y}{\partial t} + \frac{gh\partial(h+z)}{\partial y} + \frac{gn^2q^2}{hR^{4/3}} = 0, \quad (5)$$

where  $q$  is the flow per unit width,  $g$  is gravity acceleration,  $R$  is the hydraulic radius,  $z$  is the surface elevation,  $h$  is the flood water depth, and  $n$  is the friction coefficient (we used Manning's friction coefficient in this study),  $\partial x$ ,  $\partial y$  are the lengths of the grid in  $x$  and  $y$  direction, respectively.  $R$  is approximated  $h$  for wide and shallow flows, and  $\partial x$ ,  $\partial y$  are equal for raster data. Then, the equation with the step time is transformed as follows:

$$\frac{q_{t+\Delta t} - q_t}{\Delta t} + \frac{gh_t\Delta(h+z)}{\Delta x} + \frac{gn^2q_t^2}{h_t^{7/3}} = 0, \quad (6)$$

where  $q_{t+\Delta t}$  is the unit flow of  $q_t$  at the next time step and can be transformed into an explicit expression as follows:

$$q_{t+\Delta t} = \frac{q_t - gh_t\Delta t\left(\frac{\Delta(h_t+z)}{\Delta x}\right)}{1 + gh_t\Delta t n^2 q_t / h_t^{10/3}}, \quad (7)$$

To enhance the model stability, the model time step was determined using an adaptive time-stepping method [21], which is based on the Courant–Friedrichs–Lewy condition:

$$C_r = \frac{u\Delta t}{\Delta x}, \quad (8)$$

where  $C_r$  is the Courant number, which is limited to less than 1 for model stability,  $u$  is the velocity, which can be expressed as  $\sqrt{gh}$ , ignoring the advection in the shallow water flow. Therefore, the time step is limited by the following equation:

$$\Delta t_{\max} = \alpha \frac{\Delta x}{\sqrt{gh_t}}, \quad (9)$$

where the  $\alpha$  coefficient is typically defined between 0.2 and 0.7 and is set to 0.7 in this 2D model.

The primary role of the 2D model is to handle the surcharge from the SWMM. Manholes or other nodes linked to the 2D model serve as the model's source or sink points. In the simulation process, we altered the water depth of cells by the source or sink terms, and the method is shown in Equation (10). When rainwater flows back into the SWMM model, unless the time step is very small, the water in the cell can be drained in the time step, even if the water depth becomes negative. Therefore, the flow rate of the point source needs to be limited by Equation (11).

$$h_{(t+\Delta t)} = h_t + \frac{q_{ps}\Delta x}{\Delta x\Delta y}\Delta t, \quad (10)$$

$$q_{ps} = \min\left(q_{ps}, \frac{\Delta x\Delta y(h_t - h_{t+\Delta t})}{\Delta t}\right), \quad (11)$$

where  $\Delta t$  is the model time step;  $h_t$  and  $h_{t+\Delta t}$  are the cell water depths at the time  $t$  and  $t + \Delta t$ , respectively, and  $q_{ps}$  is the flow rate of the point source or sink.

### 2.1.3. Model Coupling

In the coupled model, the SWMM model simulates the primary urban drainage process, in which the 2D model handles the surcharge flow. In the coupling process, the SWMM receives rainfall and calculates the surface runoff with the hydrological model. Surface runoff after a series of hydrological processes, such as evaporation and infiltration, enters the sewer drainage system. When the runoff exceeds the drainage capacity, the surcharge will flow out the sewer network through manholes and the 2D model will simulate and display the formation and spread of surface flooding. Once the sewer network's drainage capacity is restored, the surface flooding of the 2D model will enter the SWMM again and gradually recede. Therefore, the coupled model with this coupling method is still a hydrological-hydrodynamic model.

The process of coupling models is that the two models are executed cyclically and exchange water flows at each time step until the elapsed time ( $t$ ) reaches the set simulation time ( $t_{\max}$ ), illustrated in Figure 2. For coupling flood models, the first step is to establish the links between the models, and the coupled model exchanges runoff or flow through these links. In this study, the SWMM and 2D model links are created through the junctions of SWMM, which are manholes or inlets in the sewer network, with the closest cell of the raster data in location. However, the different junctions can connect to the same cell, especially when the raster resolution is very low. The cell's connection status needs to be checked before the new link is created with it to avoid this situation. The cell will be excluded if a link already exists, and the next cell will be searched. In general, high-resolution raster data are required in urban flood models to express complex urban terrain, and the length of sewer pipes is longer than that of the cell. Therefore, a situation in which multiple manholes link to cells produces a low probability. The two coupled models are then executed individually and linked by exchanging discharge obtained at proper locations and times for appropriate linkages.

The interacting discharge is a crucial process in the coupling between the two models, and we have applied insights from several model coupling studies to our work [26,27]. The bidirectional interacting discharge is calculated according to the water level difference between the sewer network and the overland surface. The discharge between the two models was determined by comparing the hydraulic head of the maintenance hole in the SWMM ( $h_{1D}$ ), the surface water level in the 2D model ( $h_{2D}$ ), and the surface elevation ( $z_{2D}$ ). When  $h_{1D} < z_{2D}$  the rainwater flows into the maintenance hole from the surface, the discharge is calculated using the weir equation (Equation (12)). When  $h_{1D} > z_{2D} + h_{2D}$  the interacting discharge is obtained from an orifice equation (Equation (13)). If  $h_{1D} > z_{2D}$  and  $h_{1D} < z_{2D} + h_{2D}$ , the discharge is calculated using an orifice equation (Equation (14)). In this situation, the water flows into the maintenance hole.

$$q = c_w w h_{2D} \sqrt{2g h_{2D}}, \quad (12)$$

$$q = -c_o A_m \sqrt{2g(h_{1D} - z_{2D} - h_{2D})}, \quad (13)$$

$$q = c_o A_m \sqrt{2g(h_{2D} + z_{2D} - h_{1D})}, \quad (14)$$

where  $q$  is the interacting discharge,  $c_w$  is the weir discharge coefficient,  $w$  is the weir crest width,  $A_m$  is the manhole area,  $c_o$  is the orifice discharge coefficient, and  $g$  is the gravitational acceleration.

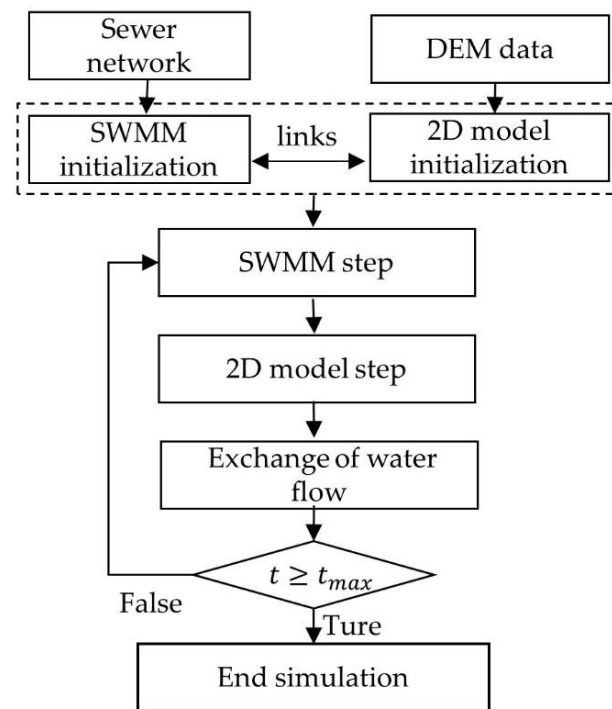


Figure 2. Flow diagram of model coupling.

Although the SWMM supports input parameters and output results in the International System of Units, in the programming code of the SWMM, the calculations are conducted using US Customary Units. However, the calculation process of the 2D model is the International System of Units. Therefore, data units used for the exchange from the SWMM are converted to the International System of Units and are consistent with the 2D model.

It is necessary to synchronize the running of the two models. The time steps in the SWMM and the 2D model are always different, although both models follow the Courant–Friedrichs–Lewy condition. The minimum time step of the coupled model is applied to the SWMM and 2D models to simultaneously maintain the two models' stability. Although a small-time step may reduce the model's efficiency, for the coupled model with the 1D SWMM and simple 2D model, the efficiency and running time of the model are still acceptable.

$$\Delta t_{couple} = \min(\Delta t_{1D}, \Delta t_{2D}), \quad (15)$$

where  $\Delta t_{1D}$  and  $\Delta t_{2D}$  are the time steps of the SWMM and 2D models, and  $\Delta t_{couple}$  is the time step used in the coupled model.

## 2.2. Study Area

We selected a 44.7 ha section of Nanjing City in China as the study area for our model (Figure 3). The area is adjacent to the Qinhuai River, which is a tributary of the Yangtze River, and less than 2 km from the Yangtze River. The area is specifically bounded by the east of Longyuanxi Road, south of Longyun Road, west of Longyuandong Road and

the Qinhuai River, and north of Longyuanbei Road. The study area is located in the city, with a high building density and significant ground surface area with low water permeability. The main land-use classes for this area are schools, residential areas, and parks. Urban flooding frequently occurs in the region and consequently, the local urban flood management department has established flood-monitoring equipment in the region. Nanjing has a subtropical monsoon climate and an annual rainfall, concentrated in the summer months of June and July, of 1200 mm. This frequent and continuous rainfall during this period of plum maturation is also called the Plum Rain season or more commonly the East Asian rainy season, as it is a commonly occurring climatic phenomenon in the middle and lower reaches of the Yangtze River.

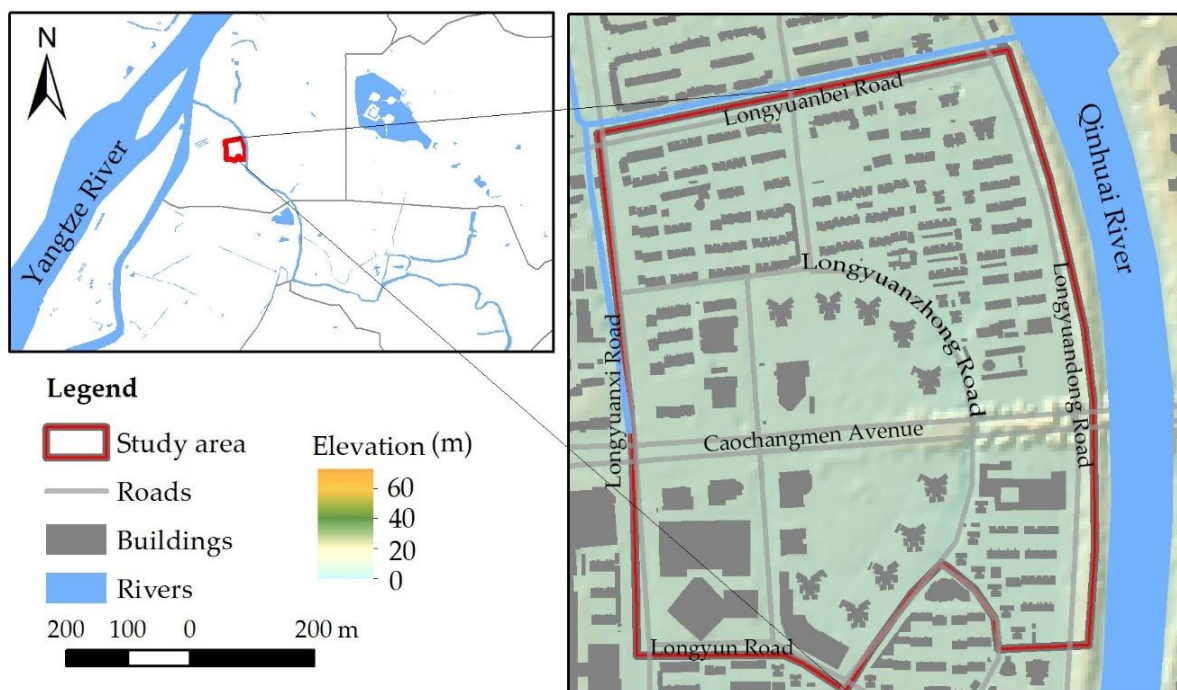


**Figure 3.** Location of the study region. The data of the figure is provided by Nanjing Planning Bureau.

### 2.3. Study Data

Abundant data are required for model building, model calibration and validation, and flood simulation with various rainfall scenarios. The following primary data were used in this study:

#### 1. Topographic data

Elevation data of 5 m resolution were obtained from a DEM of the study area from the Nanjing Planning Bureau. The building profiles were distinguished from the original DEM to represent the building blockage effect, and the building heights were added to the DEM data using GIS.

#### 2. Sewer network data

Detailed sewer network data were also obtained from the Nanjing Planning Bureau and contained geometric and corresponding attribute information of more than 7000 pipelines, junctions, and outlets. All the pipes are circular with diameters ranging from 0.15 to 2 m. Pipelines with large diameters are distributed along the roads, and pipelines with small diameters are located in residential areas. Although we attempted to retain the complete sewer network in the model and simulation, the model required simplifying. Therefore, most of the inlets and corresponding pipes were removed from the model. Finally, nine outlets, 3153 pipelines, and 3184 junctions were used in the model.

### 3. Rainfall and flooding observation data

Observation records, which are crucial for the flood model’s calibration and validation, include records of rainfall and flooding water depth. Nanjing City has installed numerous flood and rainfall observation equipment in recent years, which record water depth in places prone to flooding and precipitation. In the study area, the inundation depth was recorded by an electronic measuring device set up by the Nanjing Urban Flood Office. The device was located next to an underpass grade separation representing a typical low-lying area compared to the surrounding area (Figure 4). We obtained water depth observations and corresponding precipitation data for two rainfall events, which occurred on 10 June 2017, 8 August 2017, and 5 July 2018, respectively, as the calibration and validation data.

### 4. Rainfall scenarios

Rainfall is an essential factor stimulating urban flooding and is a crucial input parameter for flood modeling. Several rainfall scenarios were designed using the rainstorm intensity formula and the Keifer and Chu rainfall patterns to simulate the inundation conditions under different precipitation amounts. The rainstorm intensity formula is a function of rainfall intensity, duration, and frequency (return period). It is obtained from local meteorological data statistics and applied in fields such as the planning and design of municipal drainage systems. In this study, a set of rainfall events with a duration of 2 h and 1-, 5-, 10-, 20-, 50-, and 100-year return periods were generated as the urban flood scenarios for the analyses. According to the rainstorm intensity formula published by the Nanjing Urban Management Bureau [28], rainfall intensity can be inferred from the following equation:

$$q = \frac{10716.7(1 + 0.837\lg P)}{(t + 32.9)^{1.011}}, \tag{16}$$

where  $q$  is the rainfall intensity,  $t$  is the rainfall duration, and  $P$  is the return period (1, 5, 10, 20, 50, 100-year in this study).

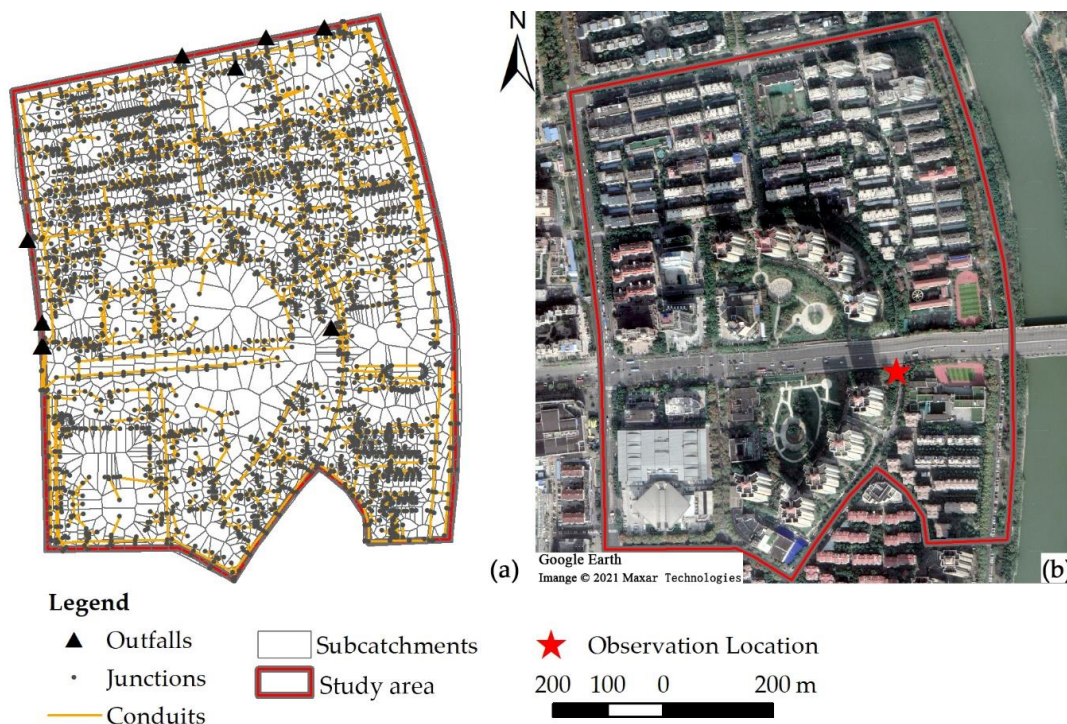


**Figure 4.** Sewer network data and flooding observation location: (a) the sewer network data sub-catchments used in the SWMM; the sub-catchments were delineated using GIS. (b) Flooding observation location.



In addition to the rainstorm intensity formula, the Keifer and Chu method, also called the Chicago method, which describes the temporal variation of rainfall intensity during a rainfall event, was developed to study rainfall flooding in Chicago [24]. The method indicates that a rainfall pattern has a peak, controlled by the peak time ratio. The rainfall intensity before and after the rainfall peak can be obtained from the following two equations:

$$i_2 = \frac{A \left[ \frac{(1-n)t_2}{r} + b \right]}{\left( \frac{t_2}{r} + b \right)^{n+1}}, \quad (17)$$

$$i_1 = \frac{A \left[ \frac{(1-n)t_1}{1-r} + b \right]}{\left( \frac{t_1}{1-r} + b \right)^{n+1}}, \quad (18)$$

where  $i_2$  and  $i_1$  are the rainfall intensities before and after the rain peak, respectively;  $t_2$ ,  $t_1$  are the time intervals before and after the rain peak;  $r$  is the rain peak time ratio ( $0 < r < 1$ ), and the  $r$  in this study is set to 0.4, which is more in line with the rainfall pattern in China [25].  $A$ ,  $b$ , and  $n$  are the local parameters in the rainstorm intensity formula based on Equation (1) and have values of 10,716.7, 32.9, and 1.011.

### 3. Results

#### 3.1. Elevation of 2D Flood Model

To evaluate the simulation capability of the raster-based 2D model (RB2D) for surface flooding caused by drainage network overflows, we design a test case based on the topographic data of the study area. In the test case, we assume an inflow point and an output point reference drainage system, respectively, and set up four gauge points between the two locations, as shown in Figure 5a. A surcharge is modeled by prescribing a 120-min inflow discharge hydrograph with a peak flow of  $1.6 \text{ m}^3/\text{s}$  illustrated in Figure 5b. The flow from the above surcharge spreads along the road. The results of the test case are compared to those obtained from LISFLOOD-FP with the acceleration solver, which has the same numerical scheme as the model used in this study.

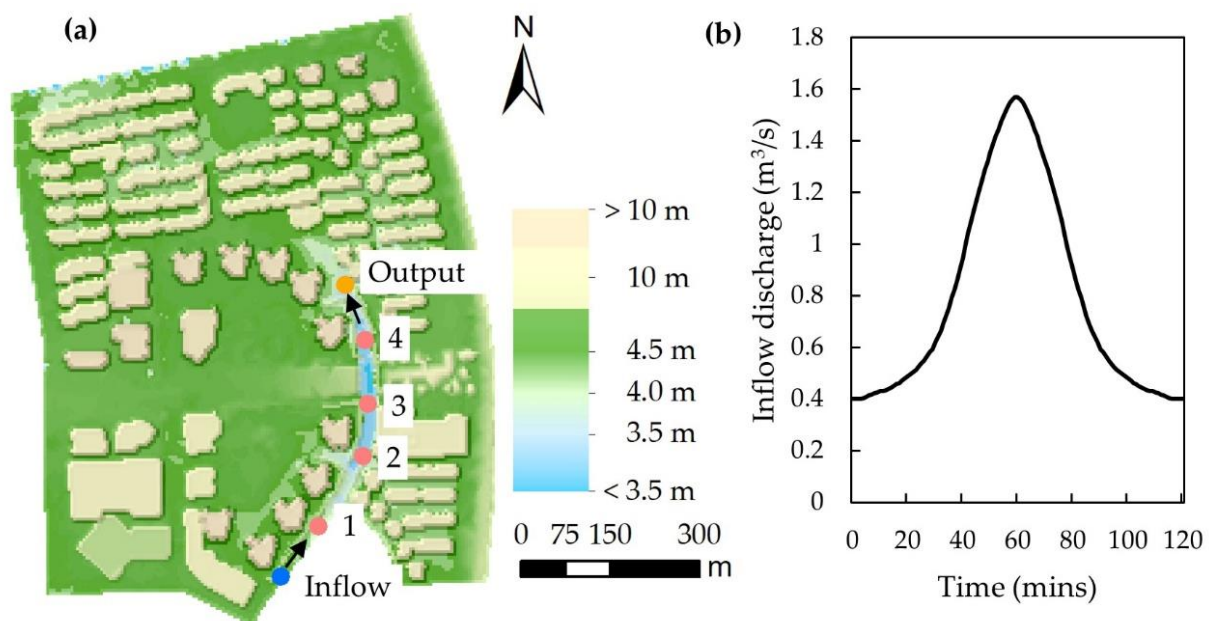


**Figure 5.** Configuration of test case: (a) terrain elevation map, with the positions of inflow, output, gauge points 1, 2, 3, and 4; (b) prescribed inflow discharge hydrograph with 120 min.

Figure 6 illustrates the water level and velocity hydrographs of the two models at the four selected locations during the simulation. The difference between the water depth results for the two models is very small most of the time, except for the slightly higher value for the 2D model at the peak in point 1. In the velocity results, the LISFLOOD-FP value is slightly higher at the peak of four points, and the results are very close at other times. In terms of model efficiency, both models take similar simulation times (LISFLOOD-FP: 15.8 s; RB2D: 16.3 s). The test results show that the 2D model is able to provide comparable capabilities to the LISFLOOD-FP model in the surface flood modeling, which has similar performance to the LISFLOOD-FP model in terms of accuracy and efficiency.

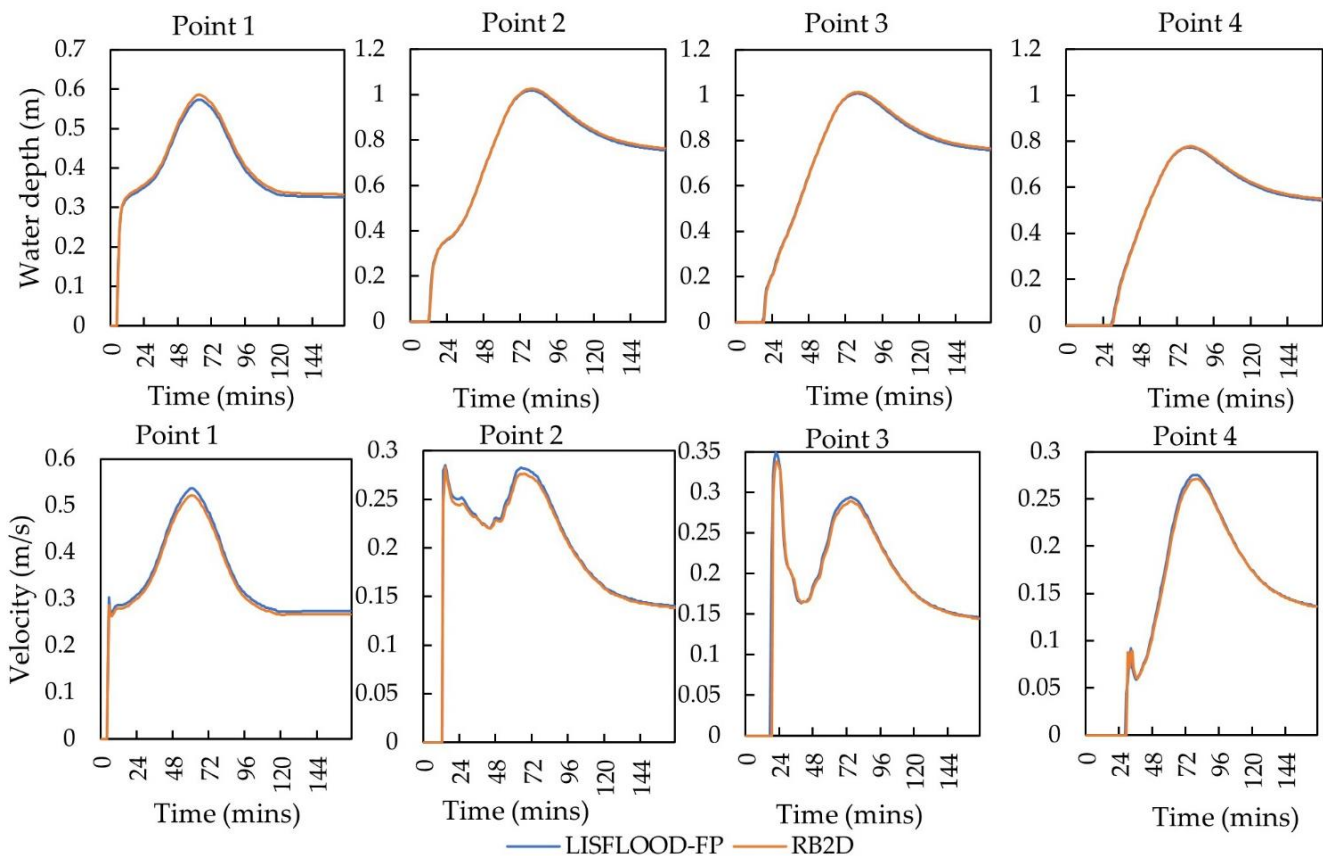


**Figure 6.** Water depth and velocity hydrographs at gauge points.

### 3.2. Model Calibration and Model Parameters

The integration model includes parameters from both the SWMM and 2D models. The parameter settings are relatively complex in the SWMM involving pipes and surface parameters. For the pipeline, the friction coefficient is an important parameter determined by the pipeline's material. In the SWMM, the surface land is divided into sub-catchments, which have many parameters that need to be set based on hydrological theory. For the 2D model, the surface land roughness is the main parameter and is determined by the type of land use [29,30]. The main model parameter settings after calibration are displayed in Table 1. The floodwater depth from the observational records and the flood modeling after parameter calibration is shown in Figure 7.

We selected three indicators to evaluate the model performance: the Nash–Sutcliffe efficiency coefficients (NSE), the coefficient of determination ( $R^2$ ), and the root mean squared error (RMSE). These evaluation methods are defined as follows:

$$NSE = 1 - \frac{\sum_{i=1}^n (h_{obs,i} - h_{mod,i})^2}{\sum_{i=1}^n (h_{obs,i} - h_{mod,mean})^2}, \quad (19)$$

$$R^2 = \frac{(\sum_{i=1}^n (h_{mod,i} - h_{mod,mean})(h_{obs,i} - h_{obs,mean}))^2}{\sum_{i=1}^n (h_{obs,i} - h_{mod,mean})^2 (h_{obs,i} - h_{obs,mean})^2}, \tag{20}$$

$$RMSE = \sqrt{\frac{1}{n} \sum_{i=1}^n (h_{obs,i} - h_{mod,i})^2}, \tag{21}$$

where  $h_{obs,i}$  and  $h_{mod,i}$  are the observed and modeling water depth at the time  $i$ , respectively, and  $h_{mod,mean}$  are the mean value of the observed and modeling water depth at the time  $i$ , respectively. The NSE is close to 1, indicating that the simulation result is closer to the observed data.

**Table 1.** Calibrated parameters for the coupled model.

Model	Parameter	Type	Value
SWMM	Manning’s n of the sewer network	Brick	0.014
		Concrete	0.014
		PVC	0.012
	Depression depth	Permeable	5 mm
	Horton infiltration	Impermeable	2.5 mm
Maximum rate		103.8 mm/h	
		Minimum rate	11.44 mm/h
2D model	Manning’s n	Building land	0.014
		Roads	0.014
		Grassland	0.24

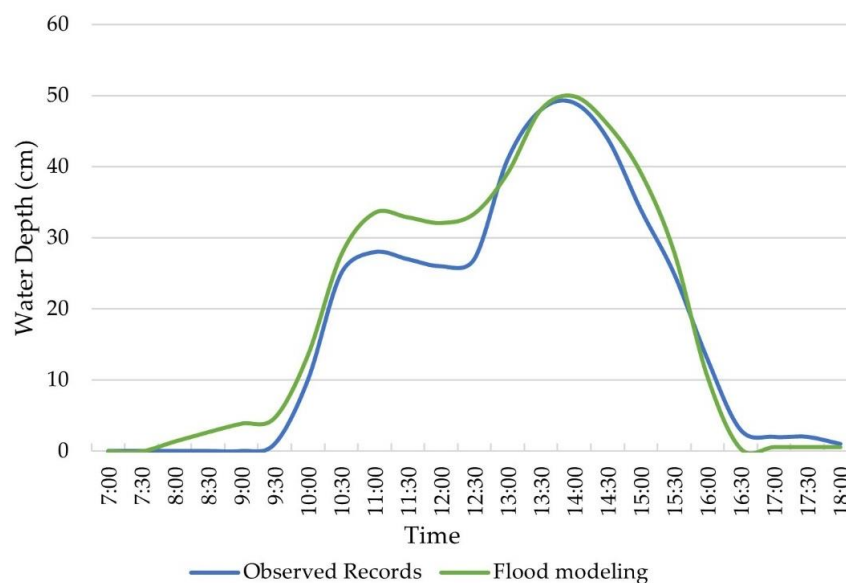


**Figure 7.** Floodwater depth from two coupling methods and observation data for the 10 June 2017, rainfall event.

We used a 10 June 2017, rainfall event to calibrate the integrated model, which lasted 6.5 h, from 7:00 to 13:30. In the flood modeling process, the total duration of the simulation was set to 11 h to simulate the complete process of urban flooding from the flood’s appearance to its gradual disappearance. Then, the observation location’s water depth was extracted from the model and compared with the observation data (Figure 7). Although the two flood models cannot replicate the rainfall event’s exact results, the flood model with calibrated parameters showed the same trend and peak time as the observation records. The NSE,  $R^2$ , and RMSE values of the model are 0.7353, 0.7439, and 8.4106, respectively. Overall, the coupled model displayed a valid result for the rainfall event, and the selected parameters were considered suitable for the case study.

### 3.3. Model Validation

After calibration, the model was validated using two rainfall events that occurred on 8 August 2017, and 5 July 2018. The comparisons of water depth from the observational data and flood modeling in two rainfalls are shown in Figure 8. The results from flood modeling and the observed records show the same trend, demonstrating that the integrated model can accurately forecast the water depth during urban flooding. Moreover, the NSE,  $R^2$  and RMSE values of the two simulations are given in Table 2. Table 2 shows that the NSE and  $R^2$  values of the two simulations are over 0.8, which can indicate that the simulation results agree well with the observations.

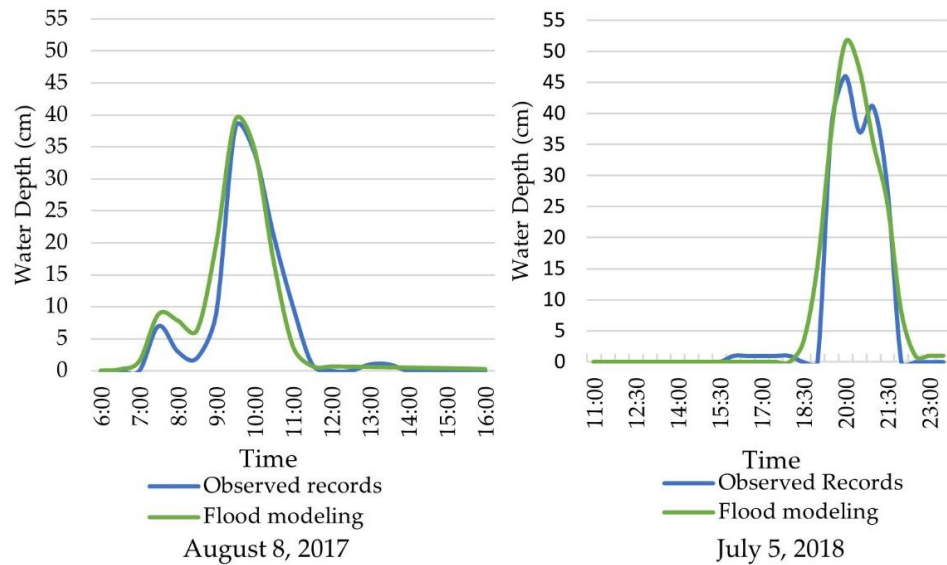


Figure 8. The inundation depth of the observation data and flood modeling.

Table 2. Validation of the simulation results and the measured data.

Rainfall Date	NSE	Maximum Water Depth (cm)		Difference (cm)	$R^2$	RMSE
		Measured	Simulated			
8 August 2017	0.8375	38	39.2	1.2	0.8626	3.6551
5 July 2018	0.8911	46	51.5	5.5	0.9049	5.7050

### 3.4. Flood Modeling with Different Rainfall Scenarios

In the scenario analyses, different urban floods 2-h durations of the 1-, 5-, 10-, 20-, 50-, and 100-year rainfall scenarios generated with the storm function and the Chicago method were simulated with the coupled model. The results of the sewer network modeling and surface flooding are displayed in Figures 9 and 10. The total surcharge volume of the manholes during sewer network modeling is shown in Figure 9. The results only demonstrate the manholes with surcharge volume exceeding 50 m<sup>3</sup>. The manholes were filtered to avoid the negative impact of excess manholes and inlet points on visualization. The distribution of maximum water depth for the various scenarios is shown in Figure 10.

For the coupled model, surface flooding was produced by surcharge from the sewer network, and the identification of surcharge nodes is an important method to improve the drainage capacity. During sewer network modeling (Figure 9), there were 3, 8, 8, 9, 9, and 9 overflow nodes with surcharges volume exceeding 1000 m<sup>3</sup> during rainfall intensities with return periods of 1-, 5-, 10-, 20-, 50-, and 100-years, respectively. More severe overflow nodes appeared as the rainfall intensity increased, most of which were distributed along the main roads. The identification of these overflow nodes can help the management of urban flooding.

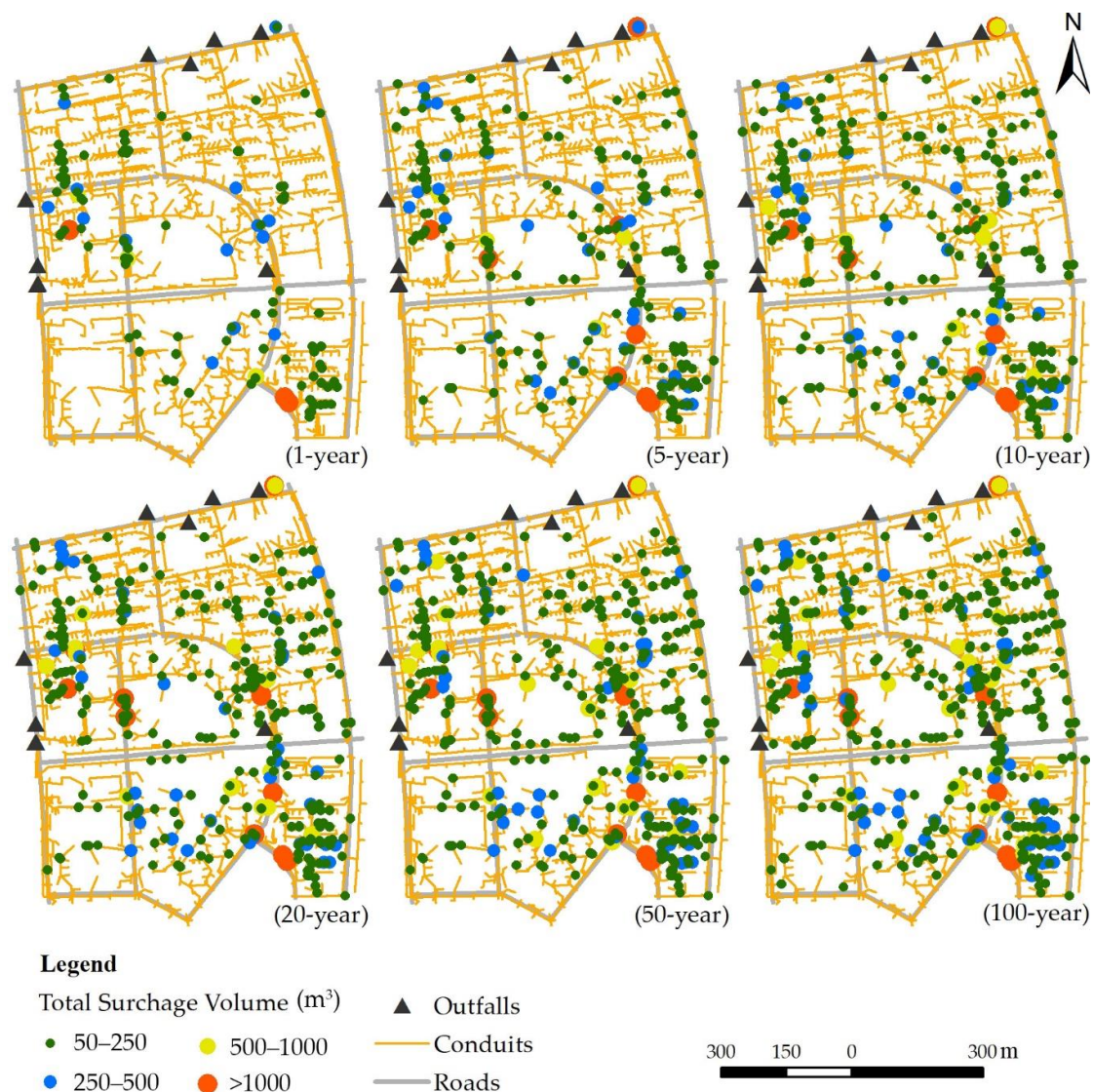


**Figure 9.** Total surcharge volume of manholes with different rainfall intensity intervals.

The coupled model not only has the capacity for sewer network modeling but can also express surface flooding. We determined from the simulation of surface flooding (Figure 10) that most of the study area might be affected by urban flooding. The flooding area initially affected low-lying areas, and the floodwater depth and extent increased gradually with an increase in rainfall intensity. There is little urban flooding area with the 1-year rainfall. However, the flooding area increased gradually with a rainfall intensity interval of >5 years. The areas least affected by flooding are situated in the southwestern portion of the study area. Longyuanzhong Road is the most affected area, with severe urban flooding occurring at a rainfall intensity interval of >5 years. Moreover, numerous roads in the residential area were affected by urban flooding, with water levels below 0.5 m. Several floods occur at the north edge of the study area, where there is a channel. However, these areas were not included in the flood model. Surface runoff flows into the channel at low elevations and generates flooding, which has little impact on residents and traffic.

From the statistics of the inundation area (Figure 11), in a 1-year rainfall scenario, the flooding area with a floodwater depth of 0.15 m or above is less than 2 ha, and this figure is approximately 14 ha when the rainfall is 100-year. For flooding areas with water depths greater than 0.15 m in all six scenarios, flooding with water depths of 0.15 m to 0.5 m occupies a major part of the flooding area. Few flooding areas exceeded the 1 m water

depth. The flooding area with a water depth of more than 1 m significantly increases as the rainfall exceeds more than 20 years, and is still a small part.

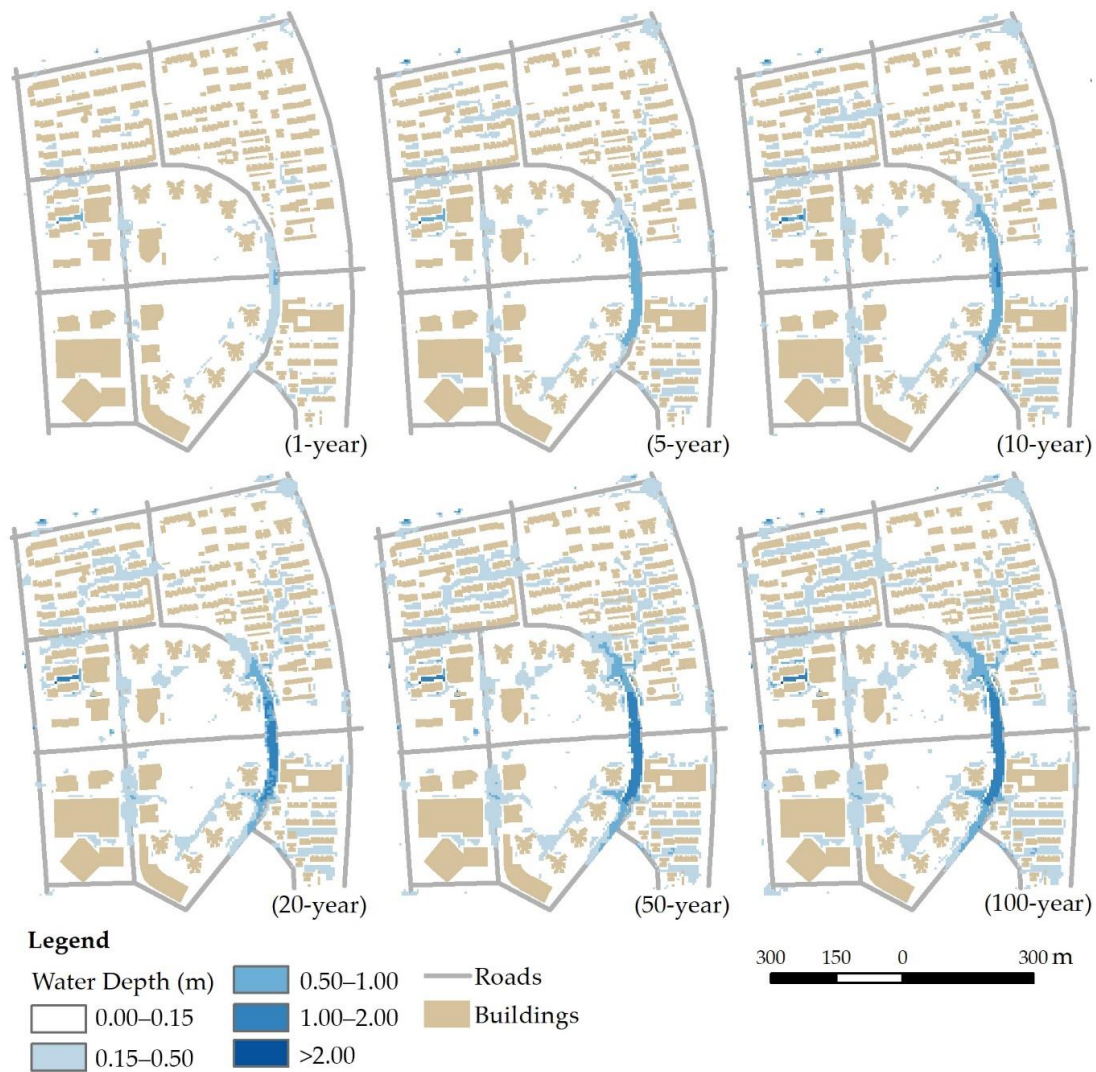


Figure 10. Maximum water depth and flooded area with different rainfall intensity intervals.

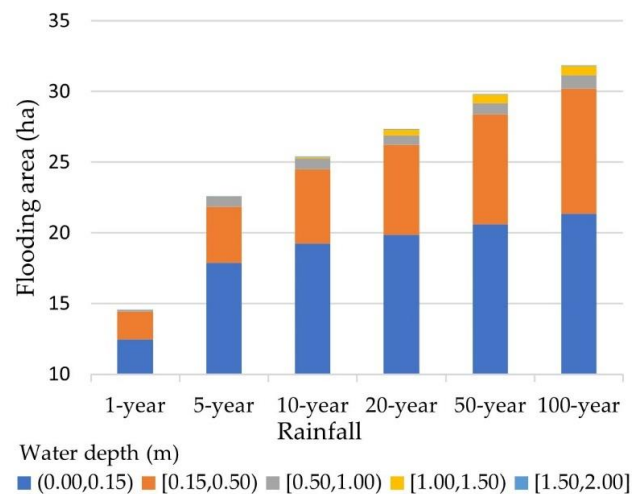


Figure 11. Inundated areas with different water depth levels.

#### 4. Discussion

This paper outlined a coupled model using SWMM and a raster-based 2D hydrodynamic model based on the simple inertial formulation of shallow water equations, for urban pluvial flood modeling. The model constructed in this study can simulate urban pluvial flooding and present two-dimensional ponding caused by the overflow of the drainage network. In the model calibration and validation, comparing the observed records revealed that the coupled model is suitable for simulation in the urban area. In addition, the use of raster data can simplify the model building process and reduce the complexity of the model. In the model, the use of GIS-based DEM data reduces the complexity of the model data structure and helps improve the efficiency of model construction in urban drainage system capacity assessment.

Calibration and validation of the model are necessary to validate its usability. However, during the model calibration and validation, the results showed several differences. For example, the observation data have a relatively long interval, and the rainfall and flooding depth have 1-h and half-hour intervals, respectively. Coarsely observed rainfall and inundation depth data restrict the accurate calibration and validation of models. Therefore, flood model simulation can produce different water depths than the observed data, and these differences are acceptable and reasonable. In this study, the model was validated in a location using the flooding water depth from the observation data, which may not adequately demonstrate the coupled model. Therefore, the model still requires further validation.

Moreover, the 2D model, whose primary purpose is to handle and demonstrate the surface flow induced by overflow from manholes, is not capable of river flood modeling. Moreover, the SWMM can simulate a complete municipal drainage system, which includes river and sewer networks. Therefore, the integrated model combined with the 2D model and the SWMM can simulate and express urban floods. Conversely, the simplified sewer network used during modeling can reduce the model's complexity and is a standard operation in the urban flood model. However, overland flood and pipe flow interaction can be affected by changes in the sewer network. These variations need to be compensated by adjusting the parameters of the model. Uncertainty parameters are not quantitatively investigated in this study. Meanwhile, model efficiency issues are not evident as the case study was conducted in a small area. When the model is applied to a large area, the model's efficiency may need to be considered and improved.

Overall, the integrated model can be used for urban flood modeling to achieve quantitative and visual simulation results. These results will help city management and policymakers assess the urban flood risk to improve urban planning, formulate and implement flood mitigation measures, and support urban residents to understand urban flood hazard characteristics.

**Author Contributions:** Conceptualization, Q.Y.; methodology and data analysis Q.Y. and Z.M.; visualization, Q.Y.; writing—original draft preparation, Q.Y.; writing—review and editing, Q.Y.; supervision, S.Z. All authors have read and agreed to the published version of the manuscript.

**Funding:** This work was supported by the National Natural Science Foundation of China (Grant Nos. 42071364, 41771424).

**Conflicts of Interest:** The authors declare no conflict of interest.

#### References

1. Mignot, E.; Li, X.; Dewals, B. Experimental modelling of urban flooding: A review. *J. Hydrol.* **2019**, *568*, 334–342. [[CrossRef](#)]
2. Zhang, W.; Villarini, G.; Vecchi, G.A.; Smith, J.A. Urbanization exacerbated the rainfall and flooding caused by hurricane Harvey in Houston. *Nature* **2018**, *563*, 384–388. [[CrossRef](#)] [[PubMed](#)]
3. Zhou, Q.; Leng, G.; Su, J.; Ren, Y. Comparison of urbanization and climate change impacts on urban flood volumes: Importance of urban planning and drainage adaptation. *Sci. Total Environ.* **2019**, *658*, 24–33. [[CrossRef](#)] [[PubMed](#)]
4. Berndtsson, R.; Becker, P.; Persson, A.; Aspegren, H.; Haghightafshar, S.; Jonsson, K.; Larsson, R.; Mobini, S.; Mottaghi, M.; Nilsson, J.; et al. Drivers of changing urban flood risk: A framework for action. *J. Environ. Manag.* **2019**, *240*, 47–56. [[CrossRef](#)]

5. Eckart, K.; McPhee, Z.; Bolisetti, T. Performance and implementation of low impact development—A review. *Sci. Total Environ.* **2017**, *607–608*, 413–432. [[CrossRef](#)]
6. Bai, Y.; Zhao, N.; Zhang, R.; Zeng, X. Storm Water Management of Low Impact Development in Urban Areas Based on SWMM. *Water* **2018**, *11*, 33. [[CrossRef](#)]
7. Chang, T.-J.; Wang, C.-H.; Chen, A.S.; Djordjević, S. The effect of inclusion of inlets in dual drainage modelling. *J. Hydrol.* **2018**, *559*, 541–555. [[CrossRef](#)]
8. Schmitt, T.G.; Thomas, M.; Ettrich, N. Analysis and modeling of flooding in urban drainage systems. *J. Hydrol.* **2004**, *299*, 300–311. [[CrossRef](#)]
9. Warsta, L.; Niemi, T.J.; Taka, M.; Krebs, G.; Haahti, K.; Koivusalo, H.; Kokkonen, T. Development and application of an automated subcatchment generator for SWMM using open data. *Urban Water J.* **2017**, *14*, 954–963. [[CrossRef](#)]
10. Vojinovic, Z.; Tutulic, D. On the use of 1D and coupled 1D-2D modelling approaches for assessment of flood damage in urban areas. *Urban Water J.* **2009**, *6*, 183–199. [[CrossRef](#)]
11. Jamali, B.; Löwe, R.; Bach, P.M.; Urich, C.; Arnbjerg-Nielsen, K.; Deletic, A. A rapid urban flood inundation and damage assessment model. *J. Hydrol.* **2018**, *564*, 1085–1098. [[CrossRef](#)]
12. Akhter, M.; Hewa, G. The Use of PCSWMM for Assessing the Impacts of Land Use Changes on Hydrological Responses and Performance of WSUD in Managing the Impacts at Myponga Catchment, South Australia. *Water* **2016**, *8*, 511. [[CrossRef](#)]
13. Pinos, J.; Timbe, L. Performance assessment of two-dimensional hydraulic models for generation of flood inundation maps in mountain river basins. *Water Sci. Eng.* **2019**, *12*, 11–18. [[CrossRef](#)]
14. Peña-Guzmán, C.A.; Melgarejo, J.; Prats, D.; Torres, A.; Martínez, S. Urban Water Cycle Simulation/Management Models: A Review. *Water* **2017**, *9*, 285. [[CrossRef](#)]
15. Türkyilmazoğlu, M. Nonlinear problems via a convergence accelerated decomposition method of Adomian. *CMES—Comput. Model. Eng. Sci.* **2021**, *127*, 1–22. [[CrossRef](#)]
16. Li, W.; Pang, Y. Application of Adomian decomposition method to nonlinear systems. *Adv. Differ. Equ.* **2020**, *2020*, 67. [[CrossRef](#)]
17. Kim, B.; Sanders, B.F.; Schubert, J.E.; Famiglietti, J.S. Mesh type tradeoffs in 2D hydrodynamic modeling of flooding with a Godunov-based flow solver. *Adv. Water Resour.* **2014**, *68*, 42–61. [[CrossRef](#)]
18. Noh, S.J.; Lee, J.-H.; Lee, S.; Kawaike, K.; Seo, D.-J. Hyper-resolution 1D-2D urban flood modelling using LiDAR data and hybrid parallelization. *Environ. Model. Softw.* **2018**, *103*, 131–145. [[CrossRef](#)]
19. Hu, R.; Fang, F.; Salinas, P.; Pain, C.C. Unstructured mesh adaptivity for urban flooding modelling. *J. Hydrol.* **2018**, *560*, 354–363. [[CrossRef](#)]
20. Geuzaine, C.; Remacle, J.-F. Gmsh: A 3-D finite element mesh generator with built-in pre- and post-processing facilities. *Int. J. Numer. Methods Eng.* **2009**, *79*, 1309–1331. [[CrossRef](#)]
21. Bates, P.D.; Horritt, M.S.; Fewtrell, T.J. A simple inertial formulation of the shallow water equations for efficient two-dimensional flood inundation modelling. *J. Hydrol.* **2010**, *387*, 33–45. [[CrossRef](#)]
22. Yin, J.; Lin, N.; Yu, D. Coupled modeling of storm surge and coastal inundation: A case study in New York City during Hurricane Sandy. *Water Resour. Res.* **2016**, *52*, 8685–8699. [[CrossRef](#)]
23. Rossman, L.A.; Huber, W. *Storm Water Management Model Reference Manual Volume II—Hydraulics*; US Environmental Protection Agency: Washington, DC, USA, 2017; p. 15.
24. Keifer, C.J.; Chu, H.H. Synthetic storm pattern for drainage design. *J. Hydraul. Div.* **1957**, *83*, 1332-1–1332-25. [[CrossRef](#)]
25. Yin, J.; Yu, D.; Yin, Z.; Liu, M.; He, Q. Evaluating the impact and risk of pluvial flash flood on intra-urban road network: A case study in the city center of Shanghai, China. *J. Hydrol.* **2016**, *537*, 138–145. [[CrossRef](#)]
26. Chen, A.S.; Leandro, J.; Djordjević, S. Modelling sewer discharge via displacement of manhole covers during flood events using 1D/2D SIPSON/P-DWave dual drainage simulations. *Urban Water J.* **2015**, *13*, 830–840. [[CrossRef](#)]
27. Leandro, J.; Martins, R. A methodology for linking 2D overland flow models with the sewer network model SWMM 5.1 based on dynamic link libraries. *Water Sci Technol* **2016**, *73*, 3017–3026. [[CrossRef](#)]
28. Bureau, N.U.M. *Nanjing Storm Intensity Formula Manual*; Nanjing Urban Management Bureau: Nanjing, China, 2014.
29. Wu, X.; Wang, Z.; Guo, S.; Liao, W.; Zeng, Z.; Chen, X. Scenario-based projections of future urban inundation within a coupled hydrodynamic model framework: A case study in Dongguan City, China. *J. Hydrol.* **2017**, *547*, 428–442. [[CrossRef](#)]
30. Yu, D.; Coulthard, T.J. Evaluating the importance of catchment hydrological parameters for urban surface water flood modelling using a simple hydro-inundation model. *J. Hydrol.* **2015**, *524*, 385–400. [[CrossRef](#)]